Contribution to IInd Aix-en-Provence International Conference on Elementary Particles

Topic: Elastic Scattering and Low Multiplicities

MEASUREMENT OF p + p → p + X BETWEEN 50 AND 400 GeV/c

K. Abe, T. De Lillo, B. Robinson, F. Sannes
Rutgers University, New Brunswick, New Jersey 08903

and

J. Carr, J. Keyne, I. Siotis
Imperial College of Science and Technology, London SW7

MEASUREMENT OF $p + p \to p + X$ BETWEEN 50 AND 400 GeV/c*

K. Abe, T. De Lillo, B. Robinson, F. Sannes
Rutgers University, New Brunswick, New Jersey 08903

and

J. Carr, J. Keyne, I Siotis
Imperial College of Science and Technology, London SW7

Abstract

We present measurements of the invariant cross section for the inclusive reaction $p + p \to p + X$ in the region $0.14 < |t| < 0.38$ GeV^2, $100 < s < 750$ GeV^2 and $0.07 < \frac{M_x^2}{s} < 0.20$

* Development and operation of hydrogen jet target supported by the State Committee for Utilisation of Atomic Energy of the USSR, Moscow. Research supported by the National Science Foundation and the Science Research Council, U.K.

In a recent letter [1] we presented the first results of our study of reaction

$$p + p \rightarrow p + X \ (1 + 2 \rightarrow 3 + X) \qquad (1)$$

using the internal H_2 jet target at the National Accelerator Laboratory. The results of Ref. (1) confirmed the phenomenon of diffractive excitation into high masses of the target (beam) particle first observed at the CERN Intersecting Storage Rings [2]. Furthermore, by studying the energy dependence of (1) for $40 \leq P_1 \leq 260$ GeV we established the presence of a large energy independent component which we identified with a non-vanishing triple Pomeron Coupling [3] for values of the momentum transfer $t = -0.33$ and -0.45 GeV^2. The results presented here extend our previous measurements to lower t values (-0.14 GeV^2) and higher energies ($P_1 = 400$ GeV). The experimental set-up is similar to the earlier experiment and is described in {1}. The main modification consisted in replacing the Aℓ absorbers which determined two momentum intervals for the recoil nucleon by a total absorption scintillation counter. The recoil proton is identified and its momentum is measured by pulse height in the 20 cm long absorption counter and time of flight over 186 cm. The resulting scatter plot of pulse height vs time-of-flight has two distinct bands corresponding to recoil protons and pions. The pulse height information is used only to remove pions. The remaining events in each 0.7 ns wide time of flight bin are summed over pulse height and represent the number of protons over the corresponding 4-momentum transfer interval. This procedure avoids the loss of proton events due to scattering in the absorption counter which leads to a broadening of the proton band. We applied a small t dependent correction to the raw data in order to take into account the loss of events due to multiple Coulomb scattering in the material in front of the total absorption counter. This correction amounted to an 8% increase at our lowest $|t|$ value and was negligible for $|t| > 0.28$ GeV^2.

Our results are expressed in terms of the invariant cross section $sd^2\sigma/dtdM^2$ which is a function of the three Lorentz invariant quantities [1]

$$s \simeq 2mE_1 \tag{2a}$$

$$t = -2m(E_3 - m) \tag{2b}$$

$$x = 1 - \frac{M_x^2}{s} \simeq (E_3 - p_3 \cos\theta_3)/m \tag{2c}$$

where s, t and M_x^2 are the squares of the centre of mass energy, the 4-momentum transfer and the missing mass. The angle between incident and recoil proton is θ_3 and m is the proton mass. Typical experimental full width resolution in these quantities are $\Delta s \simeq 30$ GeV^2, $\Delta t \simeq 0.05$ GeV^2 and $\Delta x \simeq 0.015$.

The absolute normalisation of the data presented here is obtained by monitoring the rate of elastically scattered protons in a small solid state detector [4] situated at a laboratory angle of 85.5° to the beam axis. For elastic scattering at this angle we have $|t| \simeq 0.022$ GeV^2. The pulse height spectrum in the solid state detector shows a clean elastic signal on top of a small background. Typical signal to background ratios are 20 to 1. For the rate of elastic events we have

$$N_{e\ell} = L \frac{d\sigma}{d\Omega} \Delta\Omega = \frac{L}{2\pi} \frac{d\sigma}{dt} \left(\frac{P_1}{E_1+m}\right)^2 8m^2 \cos\theta \Delta\Omega \tag{3}$$

where $\Delta\Omega$ is the solid angle subtended by the solid state detector at a laboratory angle θ to the beam. L is the luminosity and $\frac{d\sigma}{d\Omega}$ and $\frac{d\sigma}{dt}$ are the elastic differential cross sections. For $\frac{d\sigma}{dt}$ we use the form

FERMILAB-CONF-73-143-E

$$\frac{d\sigma}{dt}(s,t) = \frac{d\sigma}{dt}(s,t=0)e^{bt} \qquad (4)$$

with b(s) = 7.9 + 0.68 lns as determined in our energy range by Bartenev et al [4]. By combining eqs. (3) and (4) with the optical theorem we obtain

$$N_{e\ell} = L\,\sigma_T^2\left(\frac{mP_1}{E_1+m}\right)^2(1+\alpha^2)e^{bt}\cos\theta\Delta\Omega \qquad (5)$$

where α(s) is the ratio of real to imaginary part of the forward elastic scattering amplitude and $\sigma_T(s)$ is the total pp cross section. For α(s) we use the measurements of Ref. {4} and for $\sigma_T(s)$ we use the analytic parametrization of Bourrely and Fischer[5] which gives 38.5 mb at p_1 = 50 GeV/c and 40 mb at p_1 = 400 GeV/c in agreement with the Serpukhov [6] and CERN Intersecting Storage Rings [7] total cross section measurements [8]. Using the measured rate of elastic events we can then calculate the luminosity which allows us to obtain the overall normalisation of our data on reaction (1). It should be noted that the experimental uncertainties on α(s) and b(s) over our energy range have at most a ± 2% effect on our normalisation.

The largest uncertainty in the relative normalisation between different energies comes from $\sigma_T(s)$ for which there are no accurate measurements over our energy range. The errors in the overall normalisation of our data come mainly from uncertainties about the effective area of the solid state detector. We estimate the error on the relative normalisation between our two extreme energies to be about ± 5% while the uncertainty in the overall normalisation is about ± 15%.

Our data at five s values and four t intervals are plotted as a function of x in Figure 1. We observe a clear minimum around x = 0.88 which moves very little with s or t. We also observe a stronger energy dependence as x increases from 0.80 to 0.93. This feature is present for all four t intervals and is emphasised in Figure 2 where we plot the invariant cross section against $s^{-\frac{1}{2}}$ for x = 0.83 and 0.91. The data points can be fitted by straight lines indicating a dependence on s of the form $C(1 + \frac{B}{\sqrt{s}})$ where C and B are functions of x and t only. Finally in Figure 3 we show the invariant cross section against t for the two extreme s values with x = 0.87. The shape of the distribution can be described by a simple exponential e^{bt} with a slope b which does not change with s. This indicates that in the form $C(1 + B/\sqrt{s})$ the energy dependent term $\frac{B}{\sqrt{s}}$ is a function of x only while C is a function of x and t.

The above observations lead to a simple parametrisation for the s, t and x dependence of the data which has the form

$$\frac{s\,d^2\sigma}{dtdM^2} = A(x)e^{b(x)t}\left(1 + \frac{B(x)}{\sqrt{s}}\right) \qquad (6)$$

In Table I we give the values of A, B and b for six intervals of x.

In the limit $s \to \infty$ expression (6) reduces to Ae^{bt} and from Table I we see that at fixed t this term goes through a minimum around x = 0.88. We also not that at s = 100 GeV^2 the energy dependent part $B/\sqrt{s}$ represents 11% and 43% of the total cross section at x = 0.81 and 0.91 respectively while at s = 750 GeV^2 this part represents 4% and 16%. This implies that in order to observe any further variation in the energy range of the CERN Intersecting Storage Rings ($550 \leq s \leq 3130$ GeV^2) the relative normalisation errors between different energies must be smaller than 5%. This point emphasises the importance of the energy range $50 \leq s \leq 750$ GeV^2 in future studies of the approach to the scaling limit. A more detailed discussion of the results presented here in terms of triple

Regge couplings can be found in a separate contribution to this Conference [9].

The authors wish to thank Professor B. Maglich for his support throughout the experiment. We also acknowledge with thanks the work of J. Alspector, A. Pagnamenta and R. Stanek who made contributions at various stages of data collection and analysis. The cooperation and support of the staff of the Internal Target Laboratory at NAL is warmly acknowledged. Finally we are indebted to the members of the USSR-USA collaboration and in particular B. Morozov, S. Olsen and Y. Pilipenko for their active cooperation in sharing the use of the hydrogen gas jet target and the signals from two of their solid state detectors.

References

1. F. Sannes et al, Phys. Rev. Lett, 30, 766 (1973)

2. M. G. Albrow et al, Nuclear Physics B51, 388 (1973) and Nuclear Physics B54, 6 (1973)

3. For definitions and references see {1}

4. V. Bartenev et al, Phys. Rev. Lett. 29, 1755 (1973)

5. C. Bourrely and J. Fischer, CERN preprint TH.1652

6. S. Denisov et al, Phys. Lett. 36B, 415 (1971)

7. U. Amaldi et al, Phys. Lett. 43B, 231 (1973) and Phys. Lett. 44B, 112 (1973);
S. R. Amendolia et al, Phys. Lett. 44B, 119 (1973)

8. In reference {1} the overall normalisation was determined by extrapolating to measurements of reaction (1) at 24 and 30 GeV/c. For the relative normalisation between different energies we had assumed a constant total cross section. In view of the recent evidence for a rising total cross section a small s dependent correction should be applied to the data of reference {1}. The correction factor is simply σ_T(mb)/38.5(mb) and amounts to a 4% increase at the highest energy data of {1}

9. K. Abe et al, "Determination of triple Regge couplings from a study of reaction $p + p \to p + X$ between 50 and 400 GeV/c", paper contributed to this Conference

TABLE I

A mb/GeV^2	B GeV	b GeV^{-2}	x
77 ± 5	1.1 ± 0.7	5.7	0.81
71 ± 5	1.9 ± 0.7	5.9	0.83
64 ± 4	2.5 ± 0.7	5.9	0.85
61 ± 3	3.0 ± 0.6	5.9	0.87
62 ± 3	3.6 ± 0.5	6.0	0.89
66 ± 3	4.3 ± 0.4	6.1	0.91

FIGURE CAPTIONS

1. Invariant cross section as a function of $x = 1-M^2/s$. Statistical errors for the three intermediate energies are similar to those shown for the two extreme energies.

2. Data at fixed x plotted against $s^{-1/2}$. The straight lines are eyeball fits to illustrate the s dependence of the form $C + B/\sqrt{s}$ with a slope B which increases with x.

3. Data at fixed x plotted against t. The two extreme energies can be fitted by the same exponential $e^{5.9t}$.

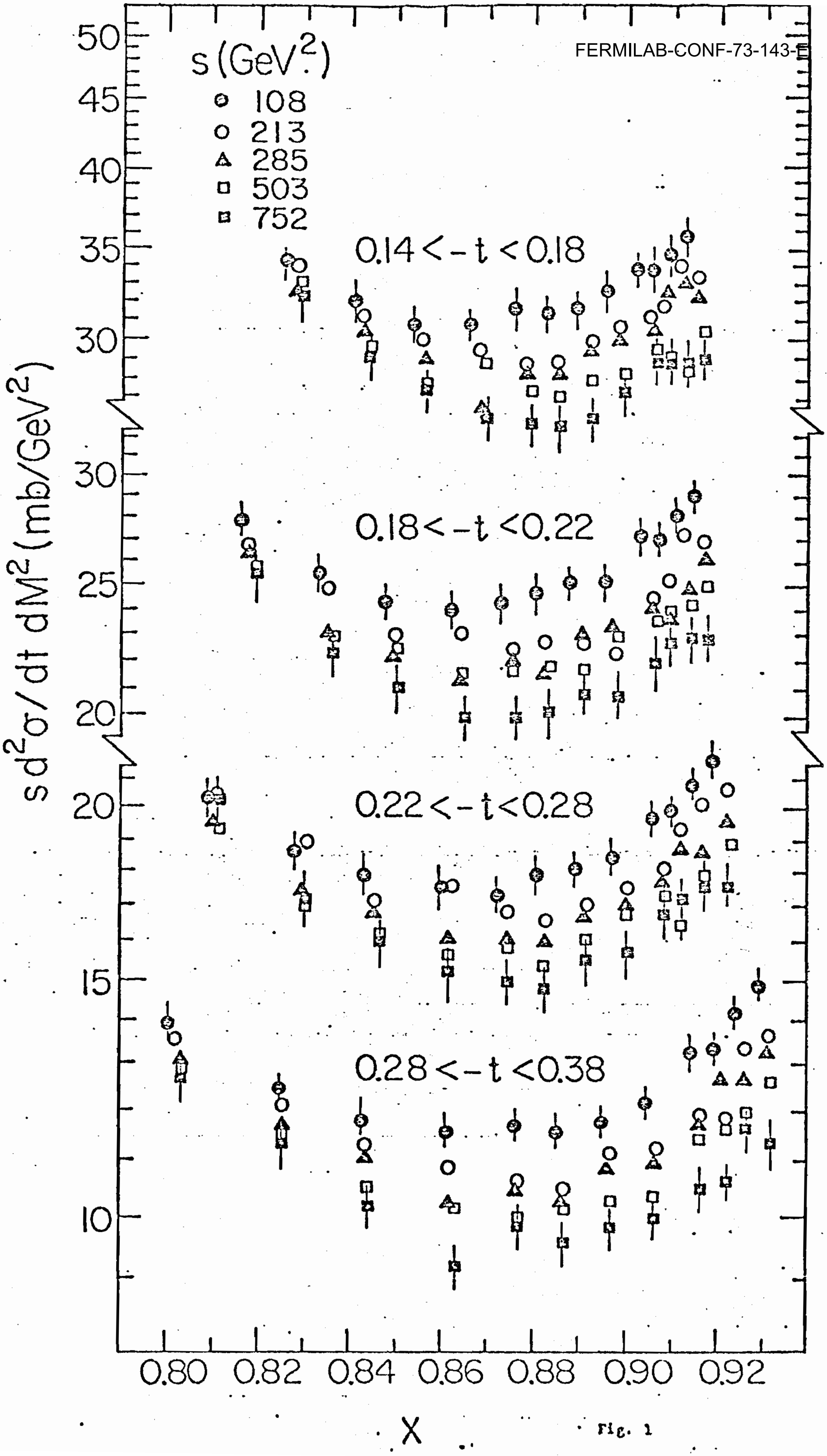
s (GeV^2)
108
213
285
503
752
0.14 < -t < 0.18
0.18 < -t < 0.22
0.22 < -t < 0.28
0.28 < -t < 0.38
s d^{2}σ/dt dM^2 (mb/GeV^2)
50
45
40
35
30
30
25
20
20
15
10
0.80
0.82
0.84
0.86
0.88
0.90
0.92
X

Fig. 1

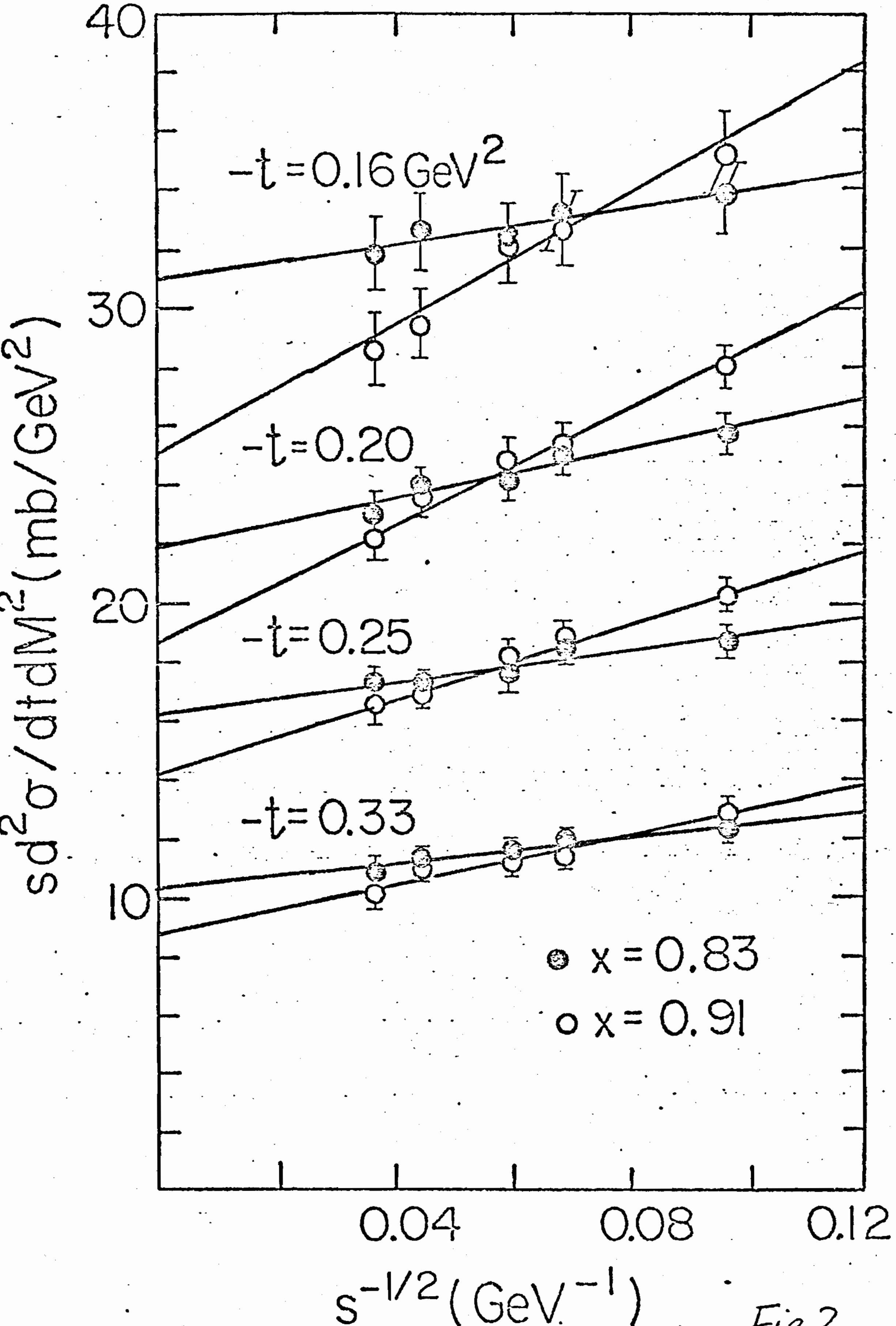
40
30
20
10
$-t = 0.16\ GeV^2$
$-t = 0.20$
$-t = 0.25$
$-t = 0.33$
$sd^2\sigma/dtdM^2$ (mb/GeV^2)
x = 0.83
x = 0.91
0.04
0.08
0.12
$s^{-1/2}$ (GeV^{-1})

Fig 2.

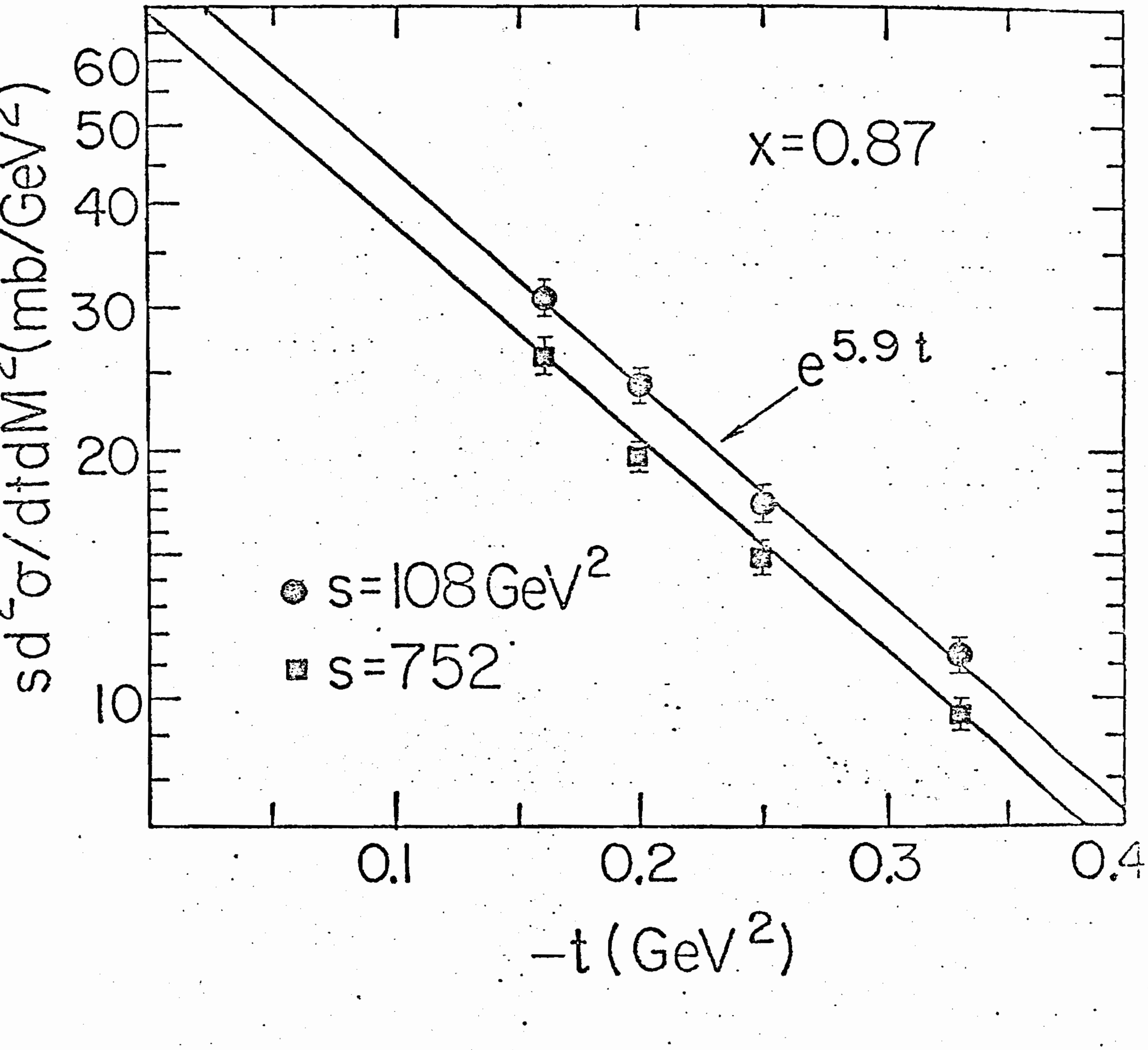

x=0.87
$e^{5.9t}$
s=108 GeV²
s=752
$sd^2\sigma/dtdM^2$ (mb/GeV²)
60
50
40
30
20
10
0.1
0.2
0.3
0.4
−t (GeV²)

Fig. 3